arXiv:hep-ph/0607095v2 27 Sep 2006

Far Field Monitoring of Rogue Nuclear Activity with an Array of Large anti-neutrino Detectors

Eugene H. Guillian*
Department of Physics, University of Hawaii, Manoa, 2505 Correa Rd., Honolulu, HI 96822, USA†
(Dated: February 2, 2008)

The result of a study on the use of an array of large anti-neutrino detectors for the purpose of monitoring rogue nuclear activity is presented. Targeted regional monitoring of a nation bordering large bodies of water with no pre-existing legal nuclear activity may be possible at a cost of about several billion dollars, assuming several as-yet-untested schemes pan out in the next two decades. These are: (1) the enabling of a water-based detector to detect reactor anti-neutrinos by doping with $GdCl_3$; (2) the deployment of a KamLAND-like detector in a deep-sea environment; and (3) the scaling of a Super-Kamiokande-like detector to a size of one or more megatons. The first may well prove feasible, and should be tested by phase-III Super-Kamiokande in the next few years. The second is more of a challenge, but may well be tested by the Hanohano collaboration in the coming decade. The third is perhaps the least certain, with no schedule for construction of any such device in the foreseeable future. In addition to the regional monitoring scheme, several global, untargeted monitoring schemes were considered. All schemes were found to fail benchmark sensitivity levels by a wide margin, and to cost at least several trillion dollars.

I. INTRODUCTION

The human race first tapped into nuclear energy with the success of the Manhattan project. Ever since, the practical know-how regarding the use of this source of energy has expanded and spread, and, so far as civilization as we know it continues to exist, this, no doubt, will continue to be the case. The spread of practical know-how in this area, however, presents a threat to peace, since there will always be desperate characters among the world's political leaders, and it is a matter of time before one such leader gets access to this know-how and decides to use it indiscriminately against his enemies.

Monitoring regimes exist to guard against the uncontrolled spread of nuclear technology and the detonation of nuclear bombs. The International Atomic Energy Agency (IAEA) works under the auspices of the United Nations to make sure that nations that use nuclear energy do so only for peaceful purposes [1]. Another monitoring regime is the Comprehensive Test Ban Treaty (CTBT), which is an agreement among nations to ban all nuclear explosions [2]. As recent world events (the detonation of a fission bomb by Pakistan in 1998, and the current political crisis involving nuclear activities in North Korea and Iran) have shown, however, neither regime has proved sufficient to curb the spread of nuclear technology nor the detonation of bombs. Clearly, the flaws in the regimes are mostly political. For instance, the detonation of nuclear bombs by Pakistan in 1998 was not against the CTBT because Pakistan is not a signatory. Also, the recent events in North Korea and Iran have little to do with monitoring techniques, but, rather, with flaws in the political process that allows headstrong political leaders to use nuclear threats as political bargaining chips.

Although much of the problems with today's monitoring regime is political, some of the political problems are abetted by insufficiencies in the monitoring techniques. For instance, in 2002, after mounting tensions with the United States and her allies, North Korea expelled United Nations inspectors and threatened to restart its nuclear facilities in Yongbyon [3]. Once the inspectors were ousted, it was impossible to tell whether or not the North Koreans had actually carried through with their threat to reprocess nuclear fuel. This scenario is made possible by the fact that the IAEA monitoring technique requires the cooperation of participants. Clearly, a more robust monitoring regime requires far-field monitoring techniques that do not depend on participant cooperation.

Such techniques are already in use to monitor nuclear explosions by the CTBT (seismology, hydroacoustics, infrasound, and radionuclide monitoring) [2], but they are useless for detecting nuclear reactor operation because a reactor burns nuclear fuel at a steady rate, and it does not release redionuclides into the environment. Far-field monitoring, however, is possible in principle using anti-neutrinos produced in nuclear fission. Indeed, the KamLAND experiment [4] detects anti-neutrinos from nuclear reactors at an average distance of about 180 km. anti-neutrinos are electrically neutral particles produced in nuclear fission; they interact with matter only via the *weak nuclear force*. Because of this, anti-neutrinos can easily travel through hundreds of kilometer of matter with almost no probability of interaction with the intervening material. This feature of the anti-neutrino makes its detection very difficult; however, given a big enough target, a sufficiently long exposure time, and a sufficiently low background level, they can be reliably detected.

The purpose of the study presented herein is to de-

†Current Address: Department of Physics, Queen's University, Stirling Hall, Kingston, ON, K7L 3N6, Canada
*Electronic address: guillian@owl.phy.queensu.ca

termine the feasibility of using anti-neutrino detection for far-field monitoring of both nuclear reactor operation and fission bomb detonations. At the most basic level, the feasibility of this technique has been established by KamLAND. However, they were helped by the very large signal due to the unusually large concentration of nuclear reactors in Japan[16]. In a realistic far-field monitoring scenario, the signal is expected to be tiny – probably much less than 100 MW_{th} (a typical commercial nuclear reactor power is about 2500 MW_{th}). We have found that a regionally targeted monitoring regime – e.g. the monitoring of nuclear reactor operations in North Korea – is may be possible at a projected cost of several billion dollars, as long as several as-yet-untested schemes pan out in the coming decade. We also considered the possibility of setting up a global array of large anti-neutrino detectors to detect surreptitious nuclear fission activity anywhere in the world. This was found to miss benchmark sensitivity levels by a wide margin, and to be unrealistic because of the prohibitive projected cost on the order of trillions of dollars.

II. ANTI-NEUTRINOS PRODUCED IN NUCLEAR FISSION

Nuclear reactors and fission bombs make use of the energy released by splitting heavy nuclei (primarily uranium and plutonium). The former are designed to keep the rate of splitting constant so that energy is released at a steady rate, whereas the latter is designed to cause the energy to be released in a very short period. In both cases, the daughter nuclei from the splitting of uranium and plutonium are unstable and undergo radioactive decay; an anti-neutrino is produced from every beta decay.

The rate of anti-neutrino production in a nuclear reactor is directly proportional to its thermal power. Each nuclear fission releases about 200 MeV (million electron volts) of thermal energy[17], which is equal to 3.2×10^{-11} Joules. A typical nuclear reactor has a thermal power of one gigawatt, or 10^9 Joules per second. The number of fissions per second required to produce this power, therefore, is 10^9 J/s divided by 3.2×10^{-11} J, which is equal to 3.1×10^{19}. Finally, since about 6 anti-neutrinos are produced per fission, we find that 1.9×10^{20} anti-neutrinos per second are produced for every one gigawatt of thermal power.

The corresponding calculation for a fission bomb proceeds similarly. The strength of a fission bomb is usually quoted in terms of its "yield", which is the mass of TNT that produces the same amount of energy. A small fission bomb has an yield of about 1000 ton of TNT, and one metric ton of TNT releases 4.18×10^9 Joules, so this bomb releases 4.18×10^{12} Joules of energy. As in the case of a nuclear reactor, each fission releases 200 MeV of energy, and 6 anti-neutrinos are produced per fission. Thus 1.30×10^{23} anti-neutrinos are released for every kilo-ton of fission bomb yield. Unlike a reactor, which releases anti-neutrinos at a steady rate, a fission bomb releases the anti-neutrino impulsively over a period of several seconds; almost no anti-neutrinos are emitted after about 10 seconds from the blast [5].

III. DETECTING ANTI-NEUTRINOS

The stuff that composes the material world is responsive to the electromagnetic force. It is this force that keeps a ball from going through one's hand when caught. anti-neutrinos, unlike ordinary stuff, are unresponsive to the electromagnetic force. Consequently, an anti-neutrino can travel through an extraordinary thickness of matter with almost zero chance of hitting stuff on its way through; the illustration of a neutrino traveling through a light-year thick block of lead is famous. They, however, do interact with matter via the weak nuclear force. This force has a strength comparable to that of the electromagnetic force, but the carriers of this force are very massive, unlike photons, the massless particles that transmit the electromagnetic force. As a result, the weak force has a very short range; an anti-neutrino interacts with matter only if it happens to pass by very close to a target particle. The chance of this happening is extraordinarily low, and this accounts for an anti-neutrino's ability to travel through large amount of matter.

The weak interaction between an anti-neutrino and matter can take place in various ways. For instance, an anti-neutrino can hit an electron that orbits an atomic nucleus, transmitting some of its momentum to it. Since an electron carries an electric charge, its motion through matter is very noticeable; a sensitive particle detector can detect the effects produced by this motion. For instance, an electron carrying several million electron-volts of energy travels faster than the speed of light in matter; this super-luminal motion creates a shock wave of electromagnetic radiation, which is referred to as the Cherenkov effect. Detectors like Super-Kamiokande [6] detect anti-neutrinos (and neutrinos) using this effect.

Another way that an anti-neutrino can be detected is via the inverse beta process, in which an anti-neutrino encounters a proton and comes out transformed into a positron, while the proton is transformed into a neutron. This is written symbolically as follows:

$$\overline{\nu_e} + p \rightarrow n + e^+ \tag{1}$$

The symbols $\overline{\nu_e}$, p, n, and e^+ stand, respectively, for anti-neutrino (electron-type), proton, neutron, and positron. In the study we performed, we considered detectors that use this process for detecting antineurtrinos. The advantages of this technique are the relatively high probability of the occurrence or the inverse beta process, and the "double-bang" signature produced by the anti-neutrino. That is, the out-going particles e^+ and n both produce signals in the detector. First, the e^+ produces a burst

of light, the amount of which is proportional to its energy (which is also closely related to the anti-neutrino's energy). This happens promptly after the transformation in Eqn. 1 takes place. The neutron, however, rattles around for tens to hundreds of microseconds (millionth of a second, which is a relatively long time in the present context) until it is eventually absorbed by a proton or a dopant like gadolinium in the target. This absorption is followed by the emission of gamma ray(s) of several million electron volts; a burst of light proportional to this energy is produced. In summary, then, an anti-neutrino interacting in this manner produces two bursts of light separated by a meter or so in distance, and tens to hundreds of microseconds in time. This double-bang signature is useful for picking out anti-neutrino events from the large background produced, for example, by radioactive contaminants in the detector. The background events produce random flashes of light, but they are not very likely to produce the double-bang signature [7].

The detection of anti-neutrinos using inverse beta decay is typically done using a liquid scintillator detector; KamLAND is an example of such a detector [4]. Liquid scintillator is used primarily because the amount of light produced by an anti-neutrino interaction event is very large compared to Cherenkov radiation produced in water; greater light yield translates to higher sensitivity (i.e. particles with lower energy are visible) and better energy resolution. In the present context, however, the required detector size is of the order of one megaton, which, for liquids, is about a cube of sides 100 m. At this scale, the use of liquid scintillator becomes impractical because of the cost; water is the only economically realistic target material. By itself, however, water cannot be used to detect the inverse beta decay process because the second "bang" in the double-bang signature is below the energy threshold. In order to make the second bang visible, the detector must be doped with an element such as gadolinium, which aggressively absorbs the produced neutron and emits gamma rays above the detector energy threshold. Because of the very large absorption cross section for thermal neutrons, only a 0.2% concentration is needed to capture 90% of the neutrons. For a 1 megaton detector, this corresponds to 200 tons of the salt $GdCl_3$ [8].

The rate of detection of anti-neutrinos from a nuclear reactor in a water detector is given by the equation below[18]:

$$\begin{aligned} N &= 3.04 \times 10^3 \text{ events} \\ &\times \left(\frac{T}{1 \text{ year}}\right) \cdot \left(\frac{M}{1 \text{ Megaton}}\right) \\ &\times \left(\frac{P}{100 \text{ MW}_{\text{th}}}\right) \cdot \left(\frac{100 \text{ km}}{D}\right)^2 \end{aligned} \quad (2)$$

This equation shows that a 100 MW_{th} nuclear reactor (about the upper limit of the power expected from a rogue nuclear reactor) at 100 km from a 1-Megaton detector exposed for 1 year produces about 3000 observable events. The number of anti-neutrino events from a fission bomb is given by:

$$\begin{aligned} N &= 2.25 \text{ events} \\ &\times \left(\frac{M}{1 \text{ Megaton}}\right) \cdot \left(\frac{100 \text{ km}}{D}\right)^2 \cdot \left(\frac{Y}{1 \text{ kton}}\right) \end{aligned} \quad (3)$$

Unlike Eqn. 2, which gives the rate of anti-neutrino detection (events per year), Eqn. 3 gives the total anti-neutrino yield over 10 seconds during which most of the anti-neutrinos are released by a fission bomb. Based on this equation, one finds only 2.25 events for a 1 kiloton bomb detonated at 100 km from a 1-Megaton detector. This may seem small, but since the events arrive in a 10-second window, the signal-to-background ratio is actually quite good. For instance, a 2500 MW_{th} reactor (typical power of a commercial reactor) 100 km away produces about 2.5 events in this time window, giving a signal-to-background ratio close to 1; at most locations, the ratio is much better than this.

Both Eqn. 2 and Eqn. 3 are somewhat optimistic because they were calculated assuming that the detector is sensitive to all values of anti-neutrino energy (the inverse beta process requires at least 1.8 MeV in anti-neutrino energy). In reality, the anti-neutrino energy probably needs to be at least 3.8 MeV to be visible by the detector. Only 58% of events have energy above this. Other data selection cuts may decrease the event rate somewhat, probably to a total efficiency of about 50%. For the sake of simplicity, we shall take the efficiency to be 100%. Any result we obtain here, therefore, will be over-optimistic by a factor of about $\sqrt{0.5}$. In other words, the actual sensitivity will be worse by about a factor of $\sqrt{2} \approx 1.4$.

IV. SHIELDING FROM COSMIC RAYS

Because anti-neutrinos interact very rarely with matter, extreme care must be taken to ensure that the signal is not overwhelmed by background noise. One way to deal with this is to increase the signal so much that it is comparable to the background. This is what is done in short-baseline reactor detectors [7] and near-field reactor monitoring detectors [5]. For some applications, however, the distance between the anti-neutrino source and the detector must be large. Since the anti-neutrino flux is inversely proportional to the square of this distance, the signal rate is tiny in these situations. To make up for this, the detector must be large and it must have a very small level of background noise.

There are two main classes of background noise: radioactivity present in and around the detector, and radioactivity produced by cosmic ray muons. The level of the former can be reduced to very low levels, thanks to decades of experience from numerous neutrino detection experiments. The latter, however, can only be reduced

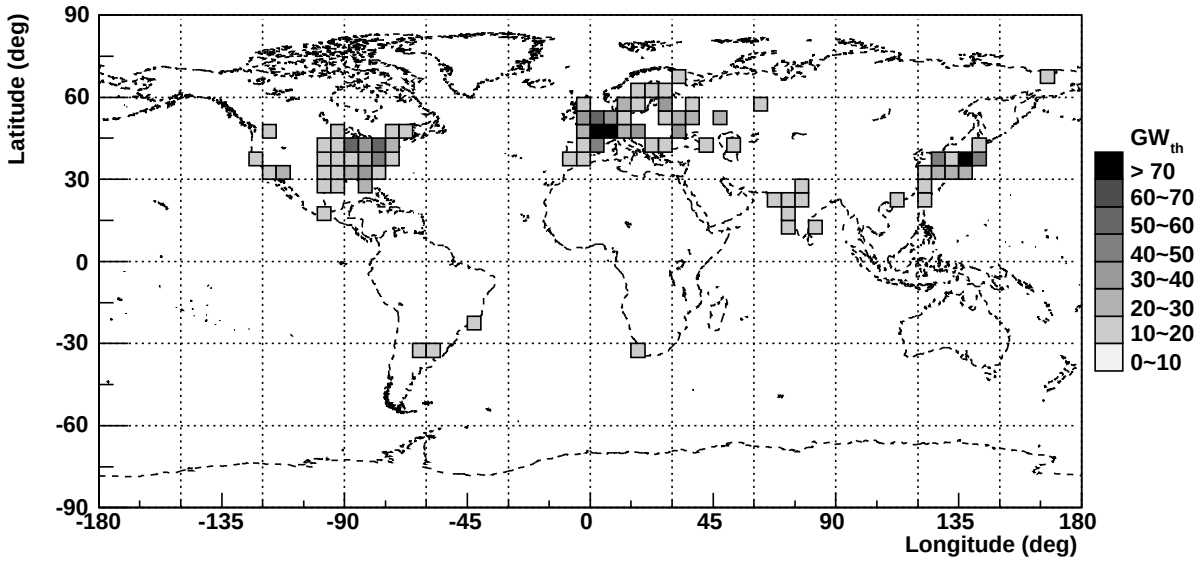

FIG. 1: A map of the thermal power of commercial and research reactors in $5^\circ \times 5^\circ$ cells on Earth.

by brute force: i.e. by having sufficient shielding material, such as rock or water. As a rough rule of thumb for typical anti-neutrino measurements, two kilometers of water is barely enough shielding, three kilometers is satisfactory, and four or more kilometers provides good shielding. Shielding by rock is very costly unless it is already present, such as inside of a pre-existing mine. Indeed, most large anti-neutrino detectors in existence today are located in commercial mines. For the purpose of nuclear monitoring, however, it is unlikely in general that commercial mines would exist in locations where the detectors need to be placed. Thus, for economic reasons, the only locations where far-field monitoring detectors could be placed are in large bodies of water (i.e. oceans, seas, and large lakes).

V. ANTI-NEUTRINO BACKGROUND SOURCES

One of the most formidable background sources for nuclear monitoring with antinuetrino detectors is the flux of anti-neutrinos from commercial and research nuclear reactors around the world. Distributed mostly around the northern hemisphere, a total thermal power of about 1 TW is produced by these reactors. The distribution of these reactors is shown in Fig. 1. See Appendix A for details on the location and power of these reactors. The number of anti-neutrinos produced by these nuclear reactors detected per year by a one-megaton detector located at various locations on Earth is shown in Fig. 2(a). anti-neutrinos produced by these reactors are virtually indistinguishable from those produced by a rogue reactor; if a rogue reactor operates in a region where the anti-neutrino flux from commercial and research reactors is high, it would be very difficult to detect.

Another possible source of background is the "georeactor", which is a hypothetical natural nuclear reactor in the core of the Earth [9, 10, 11, 12, 13]. If it exists, this reactor is expected to have a radius of several kilometers and have a thermal power of about 1 to 10 TW_{th}. Since commercial and research nuclear reactors world wide produce a total power of about 1 TW_{th}, the existence of a georeactor would have a large impact on the background rate for detecting a rogue reactor. This is illustrated in Fig. 2(b), which is the same as Fig. 2(a), but with a contribution from a 3 TW_{th} georeactor. The effect of a georeactor is not particularly serious in much of the northern hemisphere because the anti-neutrino flux is already high, but it causes a serious increase in background in much of the southern hemisphere. For this reason, a measurement of this background is an important prerequisite for the anti-neutrino detector array being considered here. A preliminary measurement has already been carried out by KamLAND [14], but the result is imprecise because of the large background from commercial nuclear reactors. However, a detector whose size is comparable to KamLAND and located far away from commercial reactors can easily make a precise measurement of georeactor power down to about 1 TW_{th}. Hanohano [15] (Hawaii anti-neutrino Observatory) is an example of a detector capable of making this measurement. Like the detectors in this array, Hanohano will be placed deep in the ocean. Thus, it is a prototype of the megaton detectors, and the successful implementation and operation of it would be an important prerequisite for the rogue activity detector array concept.

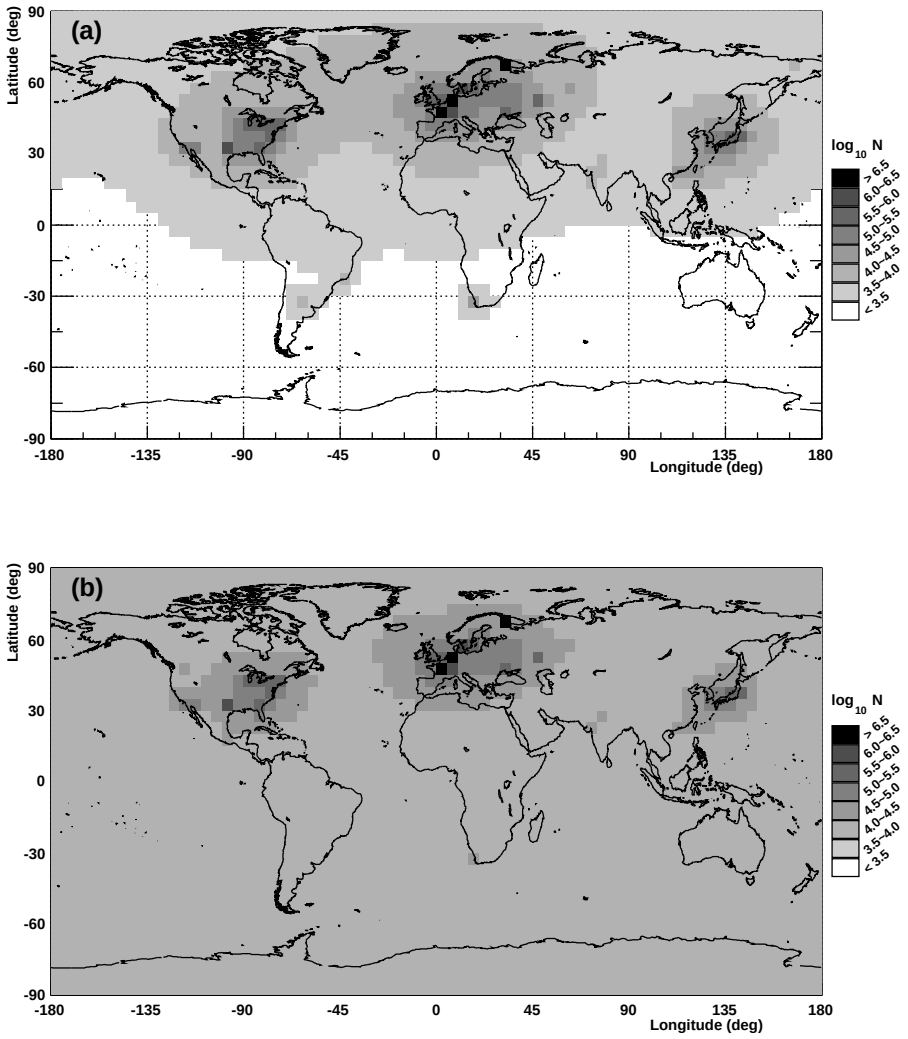

FIG. 2: The number of events per year (log scale) detected by a one-megaton anti-neutrino detector due to commercial and research reactors around the world. (a) Assuming no georeactor. (b) Assuming a 3 TW_{th} georeactor.

VI. NEUTRINO OSCILLATIONS

A potentially important detail that must be kept in mind when considering neutrino detection is neutrino flavor oscillation. The current view of the nature of neutrinos is that three "flavors" of neutrinos exist; the flavors are referred to as the "electron-type", "muon-type", and "tau-type". An electron-type neutrino turns into an electron when it interacts with the target via the charged-current electroweak interaction, while a muon-type neutrino is transformed into a muon and similarly with a tau-type neutrino. The situation with "anti-neutrinos" – which is the focus of this study – is similar, except that the out-going particle has the opposite electric charge.

The importance of the above discussion is the fact that the final state particles – the electron, muon, and the tau (and their anti-particles) – have very different masses. The electron, muon, and the tau have, respectively, a mass of 0.511, 105, and 1777 MeV. A neutrino can only undergo the charged-current interaction with the target particle if it carries at least as much energy as the out-going particle mass.

Recent results of solar and reactor neutrino experiments have unequivocally established the fact that neutrinos "oscillate". For practical purposes, this means that the neutrino flavor when it is produced is not the same as when it is detected. In the present context, electron anti-neutrinos are produced in a nuclear reactor; as these anti-neutrinos propagate outward, they become a quantum mechanical superposition of different neutrino flavors. Since these anti-neutrinos have energy well below 10 MeV, that part of the superposition that has turned into a muon- or tau-type neutrino cannot interact with the target because the available energy is insufficient to

produce a muon or tau. The result is that the anti-neutrino detection rate is smaller than is expected in the absence of neutrino oscillations. The neutrino survival probability – defined as the fraction of detection rate compared to the rate without oscillations – is a function of distance from the reactor. For a threshold energy of 1.8 MeV, this starts out at 100% for distances of 0 to several 10s of kilometers. The probability then oscillates around an asymptotic value of 0.57 as the distance ranges from about 100 km to 300 km. Beyond this, the amplitude of the oscillation approaches zero, and the probability is practically indistinguishable from 0.57.

In this study, we consider two cases: regional monitoring (section VII) and global monitoring (section VIII). In the former, the variation of the survival probability with distance affects the result of performance studies, so this has been taken into account in all figures and results. In the latter, the effect of oscillation was implemented by simply scaling the no-oscillation rate by 0.57. This simplification is valid because we are only interested in how the detector array performs as a group spanning many thousands of kilometers. In other words, in the global scheme, we are not interested in how well several nearby detectors perform (which is covered in the regional scheme), but in how well many hundreds of widely separated detectors perform. We have established that, for the global scheme, the asymptotic approximation of the survival probability is accurate to within a fraction of a percent.

VII. REGIONAL MONITORING

As an example of the capability of a megaton-scale array of anti-neutrino detectors for the purpose of detecting rogue nuclear activity, we consider a scenario in which rogue activity is taking place in North Korea. To make the illustration concrete, it was assumed that the rogue reactor is located deep inside of North Korean territory at longitude 127.0° E and latitude 40.5° N (Fig. 3(a)). North Korea presents a realistic test case not only because of recent events, but also because of the fact that it does not operate any nuclear reactors legally. If this were not the case, the monitoring regime presented here would be easily defeated because the rogue reactor could be placed close to a legally operated reactor, which would obscure this activity. Thus this monitoring regime would not be realistic for monitoring rogue activities in South Korea or Japan, or any nation with legally operating nuclear reactors.

The choice of location of anti-neutrino detectors should be based on the sensitivity to rogue reactor detection. Fig. 3 (a) shows the number of events deteced by a 1-megaton detector exposed for one year, assuming the rogue reactor power is 100 $\mathrm{MW_{th}}$.

Fig. 3 (b) shows the number of background events, mostly from commercial nuclear reactors in South Korea and Japan. The sensitivity of a detector depends on

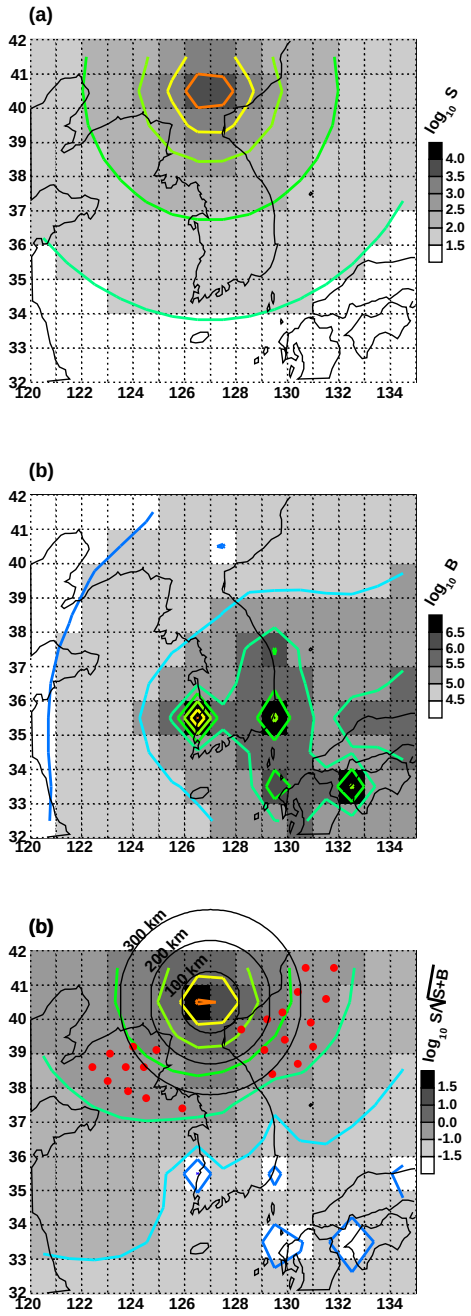

FIG. 3: The signal and background from a 100 $\mathrm{MW_{th}}$ rogue reactor deep in North Korean territory (127.0° E longitude, latitude 40.5° N latitude). (a) The signal S, defined as the number of anti-neutrino events detected by a 1-megaton detector exposed for one year. (b) The background B, defined as above, but the source of anti-neutrinos are all commercial and research reactors around the world; the vast majority of detected background comes from reactors in South Korea and Japan. (c) The signal significance $S/\sqrt{S+B}$. The dots are candidate location of the 1-megaton detectors. Eash location was chosen based on the value of the significance, whose contours are not circular because of distortions from the background.

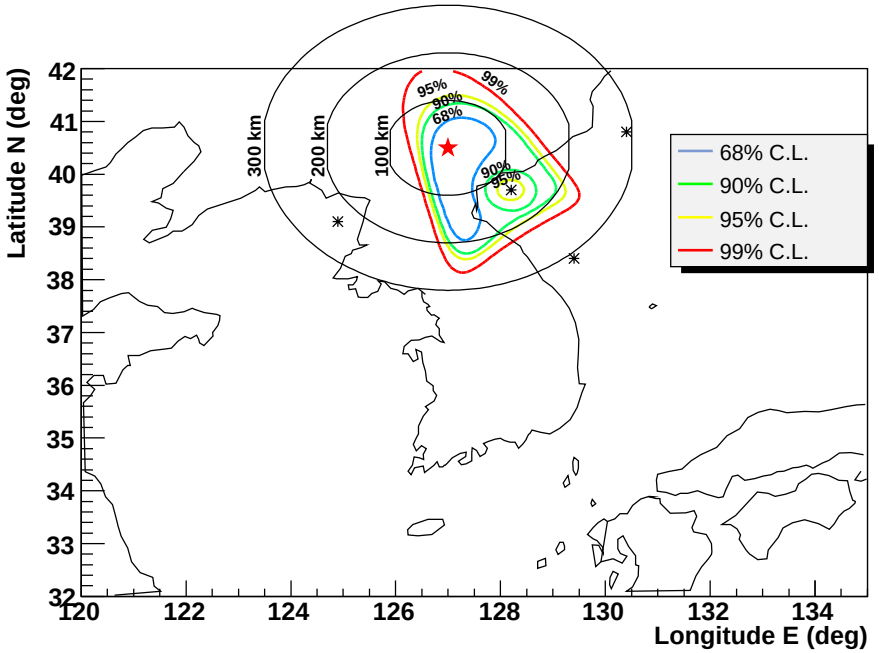

FIG. 4: This map demonstrates the ability of four 1-megaton detectors (indicated with asterisks) exposed for one year to detect and pin-point a 128 MW_{th} rogue reactor (star). The power of 128 MW_{th} corresponds to the 99% detection threshold for this configuration. It was made by varying the position and power of the unknown reactor and comparing the number of expected events with the mean number of events that would be observed for the true reactor position; the comparison was quantified using the χ^2 technique. At each longitude and latitude, χ^2 was minimized with respect to the rogue reactor power. The contours correspond to the 68, 90, 95, and 99% confidence level contour for two free parameters (longitude and latitude).

the signal S and the background B according to the formula $S/\sqrt{S+B}$. Twenty-three candidate locations were chosen based on the sensitivity contour (Fig. 3 (c)). We assumed, of course, that the detector must be located in the ocean for cosmic ray shielding. We did not consider the feasibility of the candidate locations from the point of view of political boundaries, depth, or ease of sabotage.

The general outline of the monitoring regime proceeds as follows. First, detectors are placed in several locations around North Korea. In our simulations, we examined array configurations with two to four detectors, the location of which was chosen from the 23 shown in Fig. 3 (c). Of course, we do not know the rogue reactor locaion *a priori*, but North Korea is not such a big territory, so the exact choice of locations should not matter so long as the detectors are reasonably close to land. Second, the detectors take data for about one year. During this exposure period, it receives background events from commercial reactors, but the expected level can be calculated accurately using data provided by the reactor operators. Finally, one compares the observed number of events in each detector to the expected number of background events. If a significant excess is observed in any of the detectors, an alarm is raised and one would then use the data from all the detectors to try to triangulate the location of the rogue activity. At the same time, political action would commence against the rogue regime. The statistical technique used in the comparison of the data against the background expectation is described in detail in Appendix B.

The quantity P_{99} (defined in detail in Appendix B) stands for the threshold rogue reactor thermal power that triggers an alarm at the "99%" confidence level. Fig. 4 shows an array configuration with four detectors for which $P_{99} = 128$ MW_{th}. To quantify the ability of the array to pin-point the reactor, a map of $\Delta\chi^2$ was made (Fig. 4). This map was made by comparing the observed number of events (sum of signal and background) in each detector with the number of expected events for a hypothetical rogue reactor at different locations and power levels. At each location, the power was varied until the χ^2 between the observed and expected set of events was minimized. As one would expect, the smallest *minimized* χ^2 occurs at the true reactor location; $\Delta\chi^2$ is defined as the difference between this smallest minimized χ^2 and that at any given location in the map (by definition, $\Delta\chi^2 = 0$ at the true location). The contours shown in the $\Delta\chi^2$ map indicate the range of likely reconstructed positions at the specified confidence level. In other words, an X-% contour indicates that there is an X-% chance that the reconstructed position would lie within the contour.

There are several notable features in Fig. 4. First is the fact that each detector strongly rules out a circular region of radius of several 10s km. Second is the fact that the alarm level P_{99} is determined almost completely by the closest detector. The addition of the other detectors

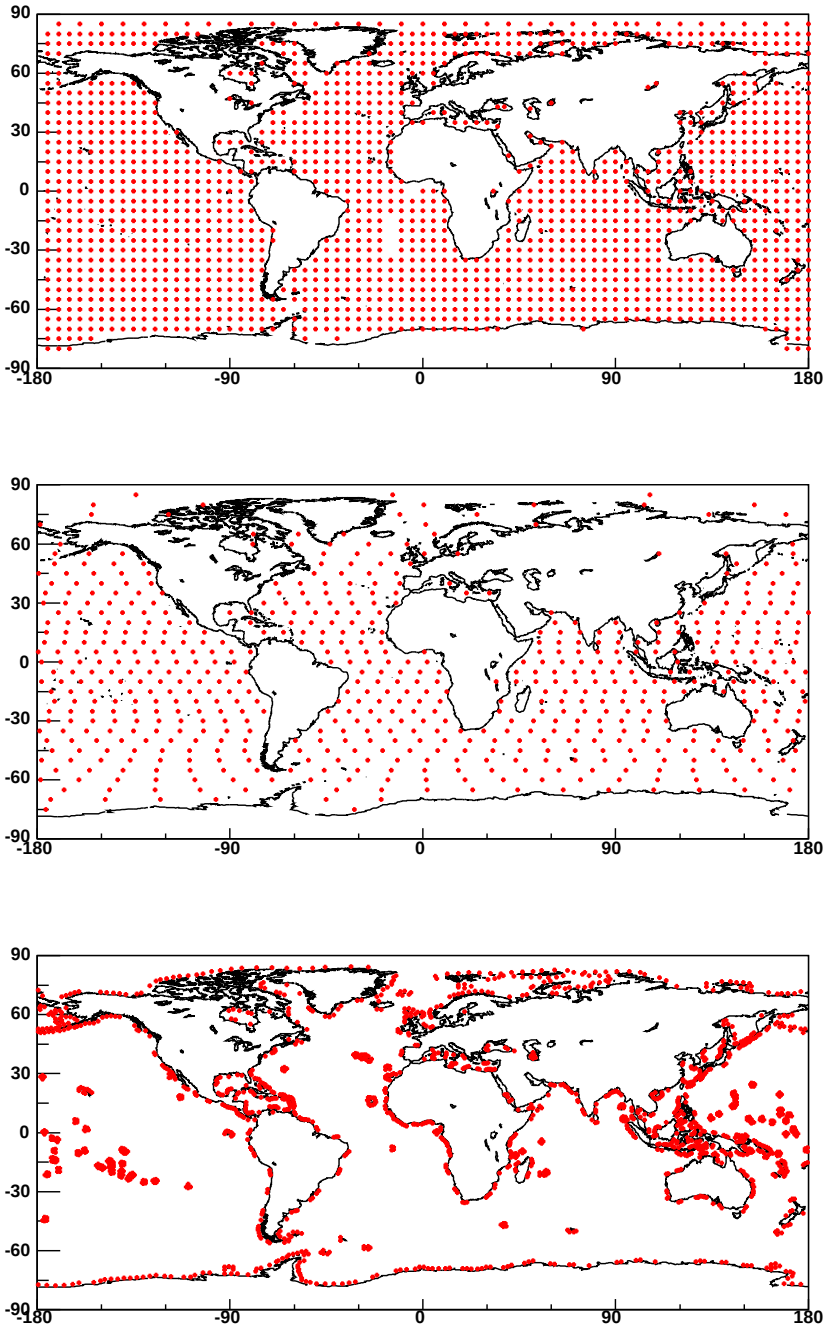

FIG. 5: The three array configurations considered in the world-wide monitoring regime. Top: detector modules distributed on a $5^\circ \times 5^\circ$ grid in longitude and latitude. Middle: modules distributed so that they are approximately equidistant from one another. Bottom: modules distributed to hug coastlines; they are approximately 100 km from land, and 100 km from each other. The number of modules in each array are 1596, 623, and 1482. The final results were normalized so that the total detector mass is equal to 1596 modules' worth.

do not lower the alarm level (i.e. they do not improve the sensitivity); their role is to help pin-point the location of the rogue reactor. To see this, note that if only the closest detector were present, the minimum χ^2 would be an annular region around it; the other detectors strongly rule out circular regions surrounding their locations, thus narrowing down the possible locations.

We finally note that nuclear reactors need to be cooled;

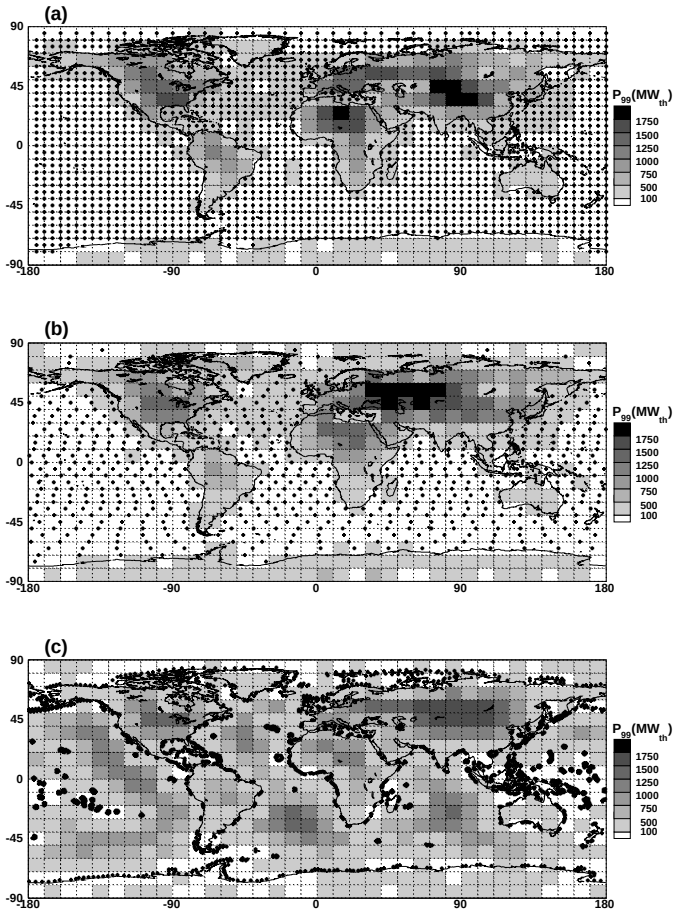

FIG. 6: Map of P_{99} for the three array configurations shown in Fig. 5. The power is in units of $\mathrm{MW_{th}}$. The number of detector modules in each array is different between arrays, but the total mass has been scaled to 1596 times 10 megatons $\approx$ 16 gigatons. The target power of $P_{99} < 100$ $\mathrm{MW_{th}}$ is indicated by the white areas.

reactors located inland are cooled with a river or a lake. Thus the intersection of rivers and lakes with the confidence region discussed above would allow one to focus in on possible reactor sites.

VIII. GLOBAL MONITORING

More ambitious in objective than regional monitoring is a global monitoring regime, the goal of which is to monitor all locations on Earth. Unlike the regional monitoring case, one cannot optimize resources to focus in on a suspect region, so the size requirements are very demanding. First, detector modules need to be an order of magnitude larger than in the regional monitoring case – i.e. each module is 10 megatons, which corresponds to a cube of sides 216 m. This is about the limiting size of a detector module from the point of view of light detection efficiency because even in extremely pure water, light has a maximum attenuation length of about 100 m [6]. Thus light produced in the center of the detector is attenuated by about a factor of 0.40; such events would be detected with low efficiency with any detector that is significantly larger. Also, the number of modules in an array needs to be on the order of 1000. As before, we took the exposure time to be one year. We considered three different array configurations in our study, shown in Fig. 5. To measure the performance of the arrays, a map of P_{99} was made (see Appendix B). In other words, a rogue reactor was assumed to exist in various locations on Earth. For each location, the rogue reactor power was varied until the reactor was detectable at the "99%" confidence level. The maps show that in most costal regions (i.e. within several hundred kilometers of the shore), the array is sensitive to rogue reactor power of several hundred $\mathrm{MW_{th}}$. The sensitivity worsens to about 1000 $\mathrm{MW_{th}}$ for regions with a high level of legal nuclear activity. The sensitivity worsens yet to almost 2000 $\mathrm{MW_{th}}$ deep within continents. Since rogue reactors, realistically, should have a power of less than about 100 $\mathrm{MW_{th}}$, it is seen that the world-wide monitoring regime considered here does not measure up well to the task at hand.

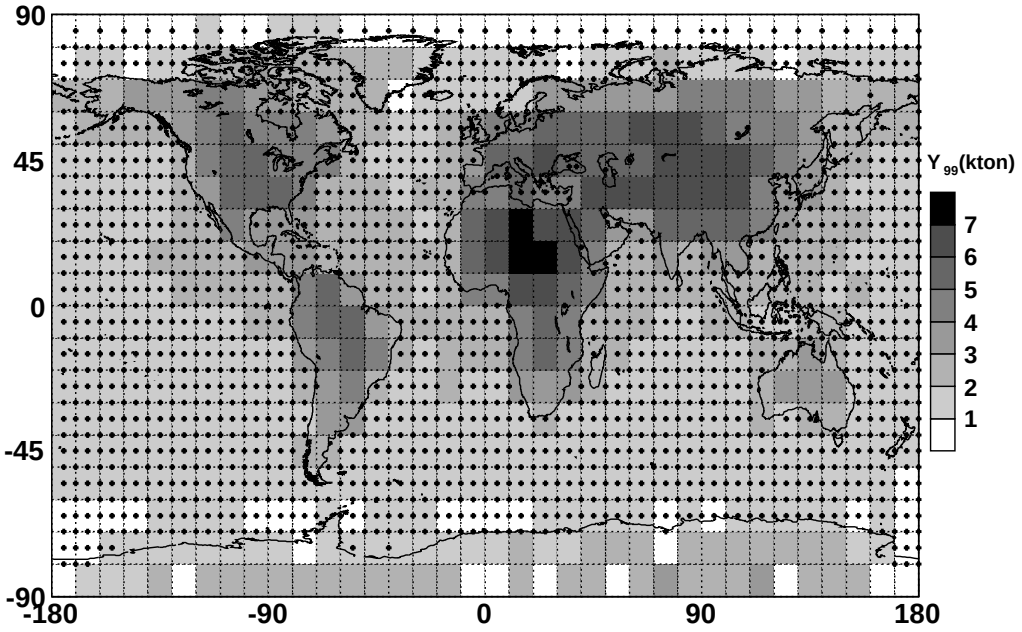

FIG. 7: Map of Y_{99} for the array configuration shown in the top of Fig. 5. The target sensitivity is less than 1 kton, which is indicated by the white boxes.

IX. MONITORING OF FISSION BOMB DETONATION

The energy production mechanism of a fission bomb is basically the same as that of a nuclear reactor. The main difference is that the latter operate in a steady-state mode, while the former releases its energy in a short burst. Most of the anti-neutrinos from a fission bomb are released in 10 seconds from the moment of detonation. The anti-neutrino yield from a 1 kton bomb observed by a 1 megaton detector at 100 km from ground-zero is 2.25 events (Eqn. 3). This may seem like a small number, but one must consider the fact that the amount of background is reduced greatly by the fact that the observation time is ten seconds. A study of the sensitivity of a global array was carried out as in the case for rogue reactors (section VIII). In this case, a map of "Y_{99}" was made instead of P_{99}, where Y_{99} is the yield of a fission bomb that can be detected at the 99% confidence level, as defined in Appendix B. The result is shown in Fig. 7. Unfortunately, at most places on Earth, the sensitivity is several kilotons, compared to the goal of one kiloton. However, since the goal is not too far off, one may achieve the goal by targeting to certain regions (though not going down quite to the regional scale like for North Korea), or by loosening the alarm threshold.

X. COST

Here, only a very rough estimate of the cost of the arrays will be attempted. The main costs involve: (1) photomultiplier tubes (PMTs), (2) detector material, civil engineering, transport, etc., (3) water purification, (4) gadolinium dopant, and (5) man-power. The PMT cost is fairly well-understood. If we assume the same coverage as the Super-Kamiokande detector (about 40% of the detector wall area), assuming that the same PMTs as Super-Kamiokande will be used, and assuming that the cost per PMT will be about \$1000 (assuming that bulk-discount or economy of scale reduces the price per PMT), about 120,000 PMT will be required per detector module. This translates to 120 million dollars per detector. The material, civil engineering, transport, etc. cost is not well-known at this point, but probably several hundred million dollars per module is the right order of magnitude. The cost of water purification is also not known right now, but probably about 100 million dollars is the right order of magnitude. Several thousand tons of $GdCl_3$ per module is required; at \$3 per kilogram, this translates to several million dollars, which is negligible compared to the total cost. Man-power and everything else is quite vague, but something on the order of \$100 million is probably the right order of magnitude. In total, then, each detector module will probably cost about \$1 billion. This implies that a regional monitoring scheme would cost several billion dollars. In contrast, a

world monitoring regime will cost several trillion dollars.

XI. CONCLUSION

Our study shows that targeted regional monitoring of rogue nuclear reactor activity in a nation without pre-existing legally operated nuclear reactor may be done at a cost of several billion dollars, provided that the nation has significant coast lines facing large bodies of water. We note, however, that the cost accounting is very rough, and that several key features of the scheme have yet to be proved feasible. For instance, the idea [8] of doping a water-based detector with gadolinium to make it sensitive to reactor anti-neutrinos is promising, but yet unproven. The verdict should be out in the next several years as Super-Kamiokande starts its third experimental phase this year (2006). Another unproven scheme is the deploying of a KamLAND-like detector in a deep-sea environment. Hanohano appears to be the single experiment that will test this idea in the coming decade. Finally, the idea of deploying a megaton-scale detector is unproven. Ideas to construct detectors on this scale exist (e.g. Hyper-K and UNO), but there are no schedules for building any. Moreover, these detectors are to be deployed on land, which probably simplifies matters considerably compared to deploying it deep in the ocean. The more ambitious idea of an untargeted world-wide array was studied, but it mostly did not reach the target sensitivity of about 100 $\mathrm{MW_{th}}$ for reactors nor the 1 kiloton yield for fission bombs. This was at a prohibitive cost of more than trillion dollars. Thus it is concluded that an untargeted world-wide monitoring scheme is unrealistic. A viable monitoring scheme must focus in on some region in order to optimize resources.

Acknowledgments

I would like to thank Prof. John Learned for his leadership in initiating at the University of Hawaii a program exploring the use of anti-neutrinos for monitoring nuclear activities. I feel honored to have been invited to join the research effort, and am indebted to him for his kind support throughout the time I was there. I would like to thank Prof. Stephen Dye for his dedication to Hanohano and related research activities. I would also like to thank Jelena Maricic for working with me on various aspects of research in anti-neutrino detection. I thank all members of the University of Hawaii Hanohano team who worked hard to keep up the momentum for an exceptionally worthy goal. Thanks also to the members of the Neutrino Physics Group and all others in the Physics Department for maintaining a high-quality research environment, and to the Department Staff whose daily support was invaluable.

APPENDIX A: A LIST OF NUCLEAR REACTOR LOCATION AND POWER

This appendix gives a list of the location (longitude and latitude) and the nominal thermal power of registered nuclear reactors throughout the world. The list was obtained in 2003 from the International Nuclear Safety Center [19]. The list may not be up to date, and the positions are only approximate. Our results, however, do not depend sensitively on the exact world wide distribution of nuclear reactors, nor on the relatively small change in the total nuclear power world wide since 2003, so this should be sufficient for the purpose of this study. A total of 433 reactors are in the list, and the total thermal power is 1.06 $\mathrm{TW_{th}}$. This list will be provided in ASCII format upon request to `ehguillian@gmail.com`.

APPENDIX B: THE STATISTICAL TECHNIQUE USED TO COMPARE THE OBSERVED NUMBER OF EVENTS AGAINST THE EXPECTED NUMBER

Let us say that there are N_{det} detectors in the array. In the absence of any rogue reactor, detector number i detects b_i events per year; these are from commercial and research reactors, and (possibly) from the georeactor in Earth's core. We denote the set of observed number of events b_1, b_2, $\ldots b_{N_{det}}$ by the usual "set" notation $\{b_i\}$.

The actually observed number of events in each detector is represented as $\{n_i\}$. In the absence of rogue activity, the numbers in $\{n_i\}$ should agree with those in $\{b_i\}$. If, however, rogue activity is taking place, the predicted numbers $\{b_i\}$ is incorrect, and it should be replaced with $\{b_i + s_i\}$, where s_i represents the number of events in detector number i due to the rogue activity.

The method used to detect rogue activity starts with the assumption that no rogue activity is taking place, so that the predicted number of events at each detector is given by $\{b_i\}$. The set of observed number of events is compared against the observed number $\{n_i\}$ using a *likelihood function*; as the name suggests, this function provides information about how likely a set of numbers $\{n_i\}$ is to have resulted from the predicted set $\{b_i\}$, given statistical and systematic uncertainties. For this report, we considered only statistical uncertainty, in which case the logarithm of the likelihood function (the log-likelihood function) is defined as follows:

$$\mathcal{L} = -b_i + n_i \ln b_i - \ln \Gamma(n_i + 1) \tag{B1}$$

The last term $\ln \Gamma(n_i+1)$ is the logarithm of the Gamma function.

The value of $\mathcal{L}$ for a given measurement (lasting one year) is not known *a priori* because of statistical fluctuations, although the mean expected value $\langle \mathcal{L} \rangle$ is (Fig. 8 (a)). The mean expected value, in fact, depends

Reactor Number	Thermal Power (MW)	Latitude	Longitude (E)	Reactor Number	Thermal Power (MW)	Latitude	Longitude (E)
1	1375	40.166	44.133	61	2894	39.200	-0.633
2	1100	-34.000	-59.250	62	3027	40.702	-2.379
3	2103	-32.233	-64.449	63	510	40.350	-2.883
4	1192	51.316	4.266	64	1	42.766	-3.200
5	1192	51.316	4.266	65	2686	39.807	-5.696
6	2775	51.316	4.266	66	2696	39.807	-5.696
7	2988	51.316	4.266	67	2686	41.200	0.566
8	2660	50.533	5.266	68	2686	41.200	0.566
9	2775	50.533	5.266	69	2785	40.966	0.883
10	2988	50.533	5.266	70	2000	61.233	21.450
11	1375	43.750	23.633	71	2000	61.233	21.450
12	1375	43.750	23.633	72	1375	60.366	26.366
13	1375	43.750	23.633	73	1375	60.366	26.366
14	1375	43.750	23.633	74	2785	45.260	-0.688
15	1882	-23.000	-44.450	75	2785	45.260	-0.688
16	2156	45.066	-66.450	76	2785	45.260	-0.688
17	2180	46.400	-72.316	77	2785	45.260	-0.688
18	2774	43.883	-78.750	78	3817	49.535	-1.881
19	2774	43.883	-78.750	79	3817	49.535	-1.881
20	2774	43.883	-78.750	80	2785	47.229	0.167
21	2774	43.883	-78.750	81	2785	47.229	0.167
22	1754	43.816	-79.066	82	2905	47.229	0.167
23	1754	43.816	-79.066	83	2905	47.229	0.167
24	1754	43.816	-79.066	84	3817	49.858	0.633
25	1754	43.816	-79.066	85	3817	49.858	0.633
26	2832	44.333	-81.600	86	3817	49.858	0.633
27	2832	44.333	-81.600	87	3817	49.858	0.633
28	2832	44.333	-81.600	88	4250	46.457	0.659
29	2832	44.333	-81.600	89	3817	44.106	0.849
30	947	46.966	7.266	90	3817	44.106	0.849
31	2806	47.366	7.966	91	3817	49.975	1.211
32	3012	47.583	8.149	92	3817	49.975	1.211
33	1130	47.550	8.216	93	2785	47.720	1.579
34	1130	47.550	8.216	94	2785	47.720	1.579
35	2905	22.600	114.533	95	2785	51.016	2.144
36	2905	22.600	114.533	96	2785	51.016	2.144
37	966	30.450	120.933	97	2785	51.016	2.144
38	1375	49.083	16.133	98	2785	51.016	2.144
39	1375	49.083	16.133	99	2785	51.016	2.144
40	1375	49.083	16.133	100	2785	51.016	2.144
41	1375	49.083	16.133	101	2785	47.733	2.516
42	3765	49.983	10.183	102	2785	47.733	2.516
43	3840	48.516	10.400	103	2785	47.733	2.516
44	3840	48.516	10.400	104	2785	47.733	2.516
45	3690	53.400	10.433	105	3817	47.507	2.877
46	2575	48.600	12.300	106	3817	47.507	2.877
47	3765	48.600	12.300	107	3817	48.517	3.520
48	3850	52.466	7.316	108	3817	48.517	3.520
49	3517	49.716	8.416	109	563	44.816	4.700
50	3733	49.716	8.416	110	2785	44.329	4.732
51	2575	49.250	8.450	111	2785	44.329	4.732
52	3850	49.250	8.450	112	2785	44.329	4.732
53	3733	53.433	8.466	113	2785	44.329	4.732
54	1050	49.366	9.083	114	2785	44.631	4.755
55	2292	53.916	9.116	115	2785	44.631	4.755
56	2497	49.033	9.166	116	2785	44.631	4.755
57	3850	49.033	9.166	117	2785	44.631	4.755
58	3765	53.850	9.350	118	3817	45.405	4.755
59	3765	52.033	9.416	119	3817	45.405	4.755
60	1892	53.616	9.533	120	4270	50.090	4.789

TABLE I: A list of registered nuclear reactors world wide.

Reactor Number	Thermal Power (MW)	Latitude	Longitude (E)	Reactor Number	Thermal Power (MW)	Latitude	Longitude (E)
121	4270	50.090	4.789	181	3293	37.416	138.600
122	2785	45.795	5.270	182	3293	37.416	138.600
123	2785	45.795	5.270	183	3293	37.416	138.600
124	2785	45.795	5.270	184	3926	37.416	138.600
125	2785	45.795	5.270	185	3926	37.416	138.600
126	3817	49.413	6.216	186	1650	43.033	140.516
127	3817	49.413	6.216	187	1650	43.033	140.516
128	3817	49.413	6.216	188	3293	36.461	140.610
129	3817	49.413	6.216	189	1380	37.416	141.000
130	2660	47.906	7.565	190	2381	37.416	141.000
131	2660	47.906	7.565	191	2381	37.416	141.000
132	1375	46.572	18.854	192	2381	37.416	141.000
133	1375	46.572	18.854	193	2381	37.416	141.000
134	1375	46.572	18.854	194	3293	37.416	141.000
135	1375	46.572	18.854	195	3293	37.316	141.033
136	660	19.833	72.700	196	3293	37.316	141.033
137	660	19.833	72.700	197	3293	37.316	141.033
138	802	21.266	73.400	198	3293	37.316	141.033
139	801	21.266	73.400	199	1593	38.400	141.500
140	801	14.866	74.450	200	2436	38.400	141.500
141	801	14.866	74.450	201	2775	35.500	126.416
142	693	24.883	75.633	202	2775	35.500	126.416
143	694	24.883	75.633	203	2825	35.500	126.416
144	801	28.183	78.366	204	2825	35.500	126.416
145	801	28.183	78.366	205	1928	35.333	129.333
146	801	12.583	80.183	206	1876	35.333	129.333
147	801	12.583	80.183	207	2775	35.333	129.333
148	1650	33.516	129.833	208	2775	35.333	129.333
149	1650	33.516	129.833	209	2775	37.100	129.383
150	3423	33.516	129.833	210	2775	37.100	129.383
151	3423	33.516	129.833	211	2825	37.100	129.383
152	2660	31.833	130.200	212	2825	37.100	129.383
153	2660	31.833	130.200	213	2156	35.750	129.500
154	1650	33.483	132.316	214	2169	35.750	129.500
155	1650	33.483	132.316	215	1000	44.600	50.300
156	2660	33.483	132.316	216	4800	55.600	26.483
157	1380	35.533	133.000	217	4800	55.600	26.483
158	2436	35.533	133.000	218	1931	19.725	-96.387
159	2440	35.516	135.500	219	1931	19.725	-96.387
160	2440	35.516	135.500	220	1366	51.433	3.716
161	2660	35.516	135.500	221	433	24.866	66.789
162	2660	35.516	135.500	222	2180	44.316	28.016
163	3423	35.533	135.650	223	62	68.033	166.250
164	3423	35.533	135.650	224	62	68.033	166.250
165	3423	35.533	135.650	225	62	68.033	166.250
166	3423	35.533	135.650	226	62	68.033	166.250
167	1031	35.683	135.966	227	3200	59.500	29.050
168	1456	35.683	135.966	228	3200	59.500	29.050
169	2440	35.683	135.966	229	3200	59.500	29.050
170	714	35.766	136.000	230	3200	59.500	29.050
171	557	35.750	136.016	231	1375	67.466	32.466
172	1064	35.747	136.022	232	1375	67.466	32.466
173	3411	35.747	136.022	233	1375	67.466	32.466
174	1593	37.050	136.733	234	1375	67.466	32.466
175	1593	34.616	138.150	235	3200	54.166	33.233
176	2436	34.616	138.150	236	3200	54.166	33.233
177	3293	34.616	138.150	237	3200	54.166	33.233
178	3293	34.616	138.150	238	3000	57.916	35.083
179	3293	37.416	138.600	239	3000	57.916	35.083
180	3293	37.416	138.600	240	3200	51.683	35.616

TABLE II: A list of registered nuclear reactors world wide (continued).

Reactor Number	Thermal Power (MW)	Latitude	Longitude (E)	Reactor Number	Thermal Power (MW)	Latitude	Longitude (E)
241	3200	51.683	35.616	301	1555	54.033	-2.916
242	3200	51.683	35.616	302	947	51.200	-3.133
243	3200	51.683	35.616	303	947	51.200	-3.133
244	1375	51.283	39.216	304	1500	51.200	-3.133
245	1375	51.283	39.216	305	1500	51.200	-3.133
246	3000	51.283	39.216	306	260	55.016	-3.216
247	3000	51.916	47.366	307	260	55.016	-3.216
248	3000	51.916	47.366	308	260	55.016	-3.216
249	3000	51.916	47.366	309	260	55.016	-3.216
250	3000	51.916	47.366	310	270	54.416	-3.483
251	60	54.233	49.616	311	270	54.416	-3.483
252	150	54.233	49.616	312	270	54.416	-3.483
253	1470	56.850	61.316	313	270	54.416	-3.483
254	2270	57.250	12.116	314	1496	54.416	-3.483
255	2440	57.250	12.116	315	1496	54.416	-3.483
256	2775	57.250	12.116	316	1760	53.416	-4.483
257	2775	57.250	12.116	317	1730	53.416	-4.483
258	1800	55.700	12.916	318	780	50.550	0.580
259	1375	57.416	16.666	319	780	50.550	0.580
260	1800	57.416	16.666	320	1550	50.550	0.580
261	3300	57.416	16.666	321	1550	50.550	0.580
262	2928	60.400	18.166	322	500	51.750	0.883
263	2928	60.400	18.166	323	500	51.750	0.883
264	3200	60.400	18.166	324	800	52.200	1.616
265	1876	45.916	15.533	325	800	52.200	1.616
266	1375	48.500	17.683	326	3411	52.200	1.616
267	1375	48.500	17.683	327	3817	33.390	-112.862
268	1375	48.500	17.683	328	3817	33.390	-112.862
269	1375	48.500	17.683	329	3817	33.390	-112.862
270	1375	48.250	18.450	330	3390	33.370	-117.557
271	1375	48.250	18.450	331	3390	33.370	-117.557
272	2785	21.966	120.733	332	3323	46.471	-119.333
273	2785	21.966	120.733	333	3338	35.212	-120.854
274	1775	25.300	121.583	334	3411	35.212	-120.854
275	1775	25.300	121.583	335	1998	41.944	-70.579
276	2894	25.200	121.666	336	3411	42.898	-70.851
277	2894	25.200	121.666	337	2700	41.309	-72.168
278	1375	51.333	25.883	338	3579	41.309	-72.168
279	1375	51.333	25.883	339	1593	42.780	-72.516
280	3000	51.333	25.883	340	3071	41.271	-73.953
281	3000	50.600	26.550	341	3025	41.271	-73.953
282	3200	51.383	30.100	342	1930	39.814	-74.206
283	3000	47.816	31.216	343	3411	39.463	-75.536
284	3000	47.816	31.216	344	3411	39.463	-75.536
285	3000	47.816	31.216	345	3293	39.468	-75.538
286	3200	47.483	34.633	346	3293	40.220	-75.590
287	3200	47.483	34.633	347	3293	40.220	-75.590
288	3200	47.483	34.633	348	3293	41.092	-76.149
289	3200	47.483	34.633	349	3293	41.092	-76.149
290	3200	47.483	34.633	350	3293	39.759	-76.269
291	3200	47.483	34.633	351	3293	39.759	-76.269
292	1500	54.650	-1.183	352	2436	43.524	-76.398
293	1500	54.650	-1.183	353	1850	43.522	-76.410
294	1555	55.966	-2.516	354	3323	43.522	-76.410
295	1555	55.966	-2.516	355	2700	38.435	-76.442
296	893	51.650	-2.566	356	2700	38.435	-76.442
297	893	51.650	-2.566	357	2441	37.166	-76.698
298	1500	54.033	-2.916	358	2441	37.166	-76.698
299	1500	54.033	-2.916	359	2568	40.153	-76.725
300	1556	54.033	-2.916	360	1520	43.292	-77.309

TABLE III: A list of registered nuclear reactors world wide (continued).

Reactor Number	Thermal Power (MW)	Latitude	Longitude (E)	Reactor Number	Thermal Power (MW)	Latitude	Longitude (E)
361	2893	38.061	-77.791	421	2568	35.227	-93.231
362	2893	38.061	-77.791	422	2815	35.227	-93.231
363	2416	33.958	-78.011	423	1670	45.333	-93.848
364	2436	33.958	-78.011	424	2381	40.362	-95.641
365	2775	35.633	-78.956	425	3411	38.239	-95.689
366	2300	34.405	-80.159	426	3817	28.795	-96.048
367	2700	27.349	-80.246	427	3817	28.795	-96.048
368	2700	27.349	-80.246	428	1500	41.521	-96.077
369	2200	25.435	-80.331	429	3411	32.298	-97.785
370	2200	25.435	-80.331	430	3411	32.298	-97.785
371	2652	40.622	-80.434	431	2775	-33.650	18.416
372	2652	40.622	-80.434	432	2775	-33.650	18.416
373	3411	35.432	-80.948	433	0	40.166	44.133
374	3411	35.432	-80.948				
375	3411	35.051	-81.069				
376	3411	35.051	-81.069				
377	3579	41.801	-81.143				
378	2775	34.296	-81.320				
379	3565	33.142	-81.765				
380	3565	33.142	-81.765				
381	2436	31.934	-82.344				
382	2436	31.934	-82.344				
383	2544	28.957	-82.699				
384	2568	34.792	-82.899				
385	2568	34.792	-82.899				
386	2568	34.792	-82.899				
387	2772	41.597	-83.086				
388	3292	41.963	-83.259				
389	3411	35.603	-84.790				
390	3411	35.223	-85.088				
391	3411	35.223	-85.088				
392	2652	31.223	-85.112				
393	2652	31.223	-85.112				
394	2530	42.322	-86.315				
395	3250	41.976	-86.566				
396	3411	41.976	-86.566				
397	3293	34.704	-87.119				
398	3293	34.704	-87.119				
399	3292	34.704	-87.119				
400	1518	44.281	-87.536				
401	1518	44.281	-87.536				
402	1650	44.343	-87.536				
403	3411	41.244	-88.229				
404	3411	41.244	-88.229				
405	2527	41.390	-88.271				
406	2527	41.390	-88.271				
407	3323	41.244	-88.671				
408	3323	41.244	-88.671				
409	2894	40.172	-88.834				
410	3411	42.075	-89.282				
411	3411	42.075	-89.282				
412	2511	41.726	-90.310				
413	2511	41.726	-90.310				
414	3410	29.995	-90.471				
415	3833	32.008	-91.048				
416	2894	30.757	-91.332				
417	1658	42.101	-91.777				
418	3565	38.758	-91.782				
419	1650	44.619	-92.633				
420	1650	44.619	-92.633				

TABLE IV: A list of registered nuclear reactors world wide (continued).

on the power P of the rogue reactor; we denote this dependence as $\langle\mathcal{L}\rangle(P)$. As the power increases, the assumption that no rogue reactor exists becomes increasingly inconsistent with observations; this inconsistency causes $\langle\mathcal{L}\rangle$ to be biased to lower values. When P is small, the slightly biased distribution of $\langle\mathcal{L}\rangle(P)$ largely overlaps the distribution of $\langle\mathcal{L}\rangle(0)$, which implies that the detector array is not sensitive enough to detect such a low value of P (Fig. 8 (b)). However, as the power is raised, a point is reached where the two distributions are different enough that the rogue reactor can be judged to exist with great confidence (Fig. 8 (c)).

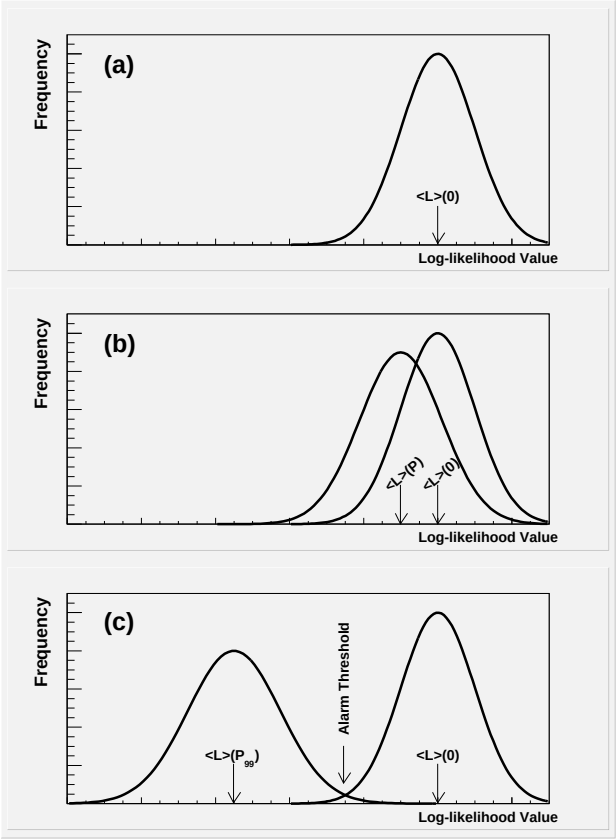

FIG. 8: Illustrating how the log-likelihood distribution changes with rogue reactor power. (a) When no rogue reactor exists, the data agree well with the assumption, so that the mean log-likelihood value $\langle\mathcal{L}\rangle(0)$ is high. Any given measurement is distributed around the mean due to statistical fluctuations. (b) As the rogue reactor power increases to P, the mean value $\langle\mathcal{L}\rangle(P)$ decreases. However, P is small so the distribution at this power largely overlaps with the distribution at zero power, which means that the detector array is not sensitive enough to confidently detect the rogue reactor. (c) When the rogue reactor power is sufficiently large, the overlap between the distributions become very small, and the existence of the reactor can be confirmed with great confidence. The power P_{99} is defined as the power above which there is 99% chance that the likelihood value will be above the alarm threshold, which is defined as the log-likelihood value below which there is only 1% chance for a "false positive". We note that the width of the distribution increases slowly with power.

For the purpose of identifying a rogue reactor, a threshold level of the log-likelihood value for triggering an alarm is necessary. If this is set too close to $\langle\mathcal{L}\rangle(0)$, the observed value of $\langle\mathcal{L}\rangle$ would easily trigger a false-positive alarm just from statistical fluctuations. For the purpose of the present study, we decided to tolerate a 1% false-positive probability (Fig. 8 (c)). Once this threshold is set, we can talk about the sensitivity of an array. We quantified this with P_{99}, which is the rogue reactor power that has a 99% chance of clearing the alarm threshold. Since rogue reactors are not likely to be much larger than 100 $\mathrm{MW_{th}}$, a promising detector array should have P_{99} at this level. Of course, the tolerance for false-positives and -negatives chosen here are arbitrary; looser tolerance would result in sensitivity to lower power, but at the cost of greater chance of mis-identification and missing an actually existing reactor.

[1] http://www.iaea.org/.
[2] http://www.fas.org/nuke/control/ctbt/.
[3] http://www.cnn.com/2005/WORLD/asiapcf/02/10/nkorea.timeline/index.html.
[4] K. Eguchi et al., Physical Review Letters **90**, 021802 (2003), URL http://www.citebase.org/cgi-bin/citations?id=oai:arXiv.org:
[5] A. Bernstein, T. West, and V. Gupta, *An assessment of antineutrino detection as a tool for monitoring nuclear explosions*, Science & Global Security, Volume 9, pp. 235-255, ©2001 Taylor and Francis.
[6] S. Fukuda et al., Nuclear Instruments and Methods in

Physics Research A **501**, 418462 (2003).
[7] C. Bemporad, G. Gratta, and P. Vogel, Reviews of Modern Physics **74**, 297 (2002), URL http://www.citebase.org/cgi-bin/citations?id=oai:arXiv.org:hep-ph/0107277.
[8] J. F. Beacom and M. R. Vagins, Physical Review Letters **93**, 171101 (2004), URL http://www.citebase.org/cgi-bin/citations?id=oai:arXiv.org:hep-ph/0309300.
[9] J. M. Herndon, Proc. R. Soc. London A **368**, 495 (1979).
[10] J. M. Herndon, Proc. R. Soc. London A **372**, 149 (1980).
[11] J. M. Herndon, Proc. Natl. Acad. Sci. USA **93**, 646 (1996).
[12] D. F. Hollenbach and J. M. Herndon, Proc. Natl. Acad. Sci. USA **98**, 11085 (2001).
[13] J. M. Herndon, Proc. Natl. Acad. Sci. USA **100**, 3047 (2003).
[14] J. Maricic, Ph.D. thesis, University of Hawaii, Manoa (2005).
[15] http://www.phys.hawaii.edu/ sdye/hnsc.html.
[16] As of 2002, Japan has 16 nuclear reactor plants producing a total power of 130 GW_{th} [7].
[17] One electron volt is the amount of energy that an electron gains when it moves from the "−" to "+" terminal of a 1-volt battery. The energy released by nuclear fission, therefore, is hundreds of million times as large as the energy released by a typical battery used in every-day life
[18] This paper assumes 100% efficiency above the threshold anti-neutrino energy of 1.8 MeV. The anti-neutrino energy spectrum depends somewhat on the relative fraction of isotopes in a fission reactor; we took average values used in [4], which were 0.567, 0.078, 0.297, and 0.057 for ^{235}U, ^{238}U, ^{239}Pu, and ^{241}Pu, respectively. The rate also depends on the production cross section for the inverse beta process; the energy dependence was taken to be the same as that used in [4]. Finally, it was assumed that all isotopes produce 204 MeV of thermal energy per fission; in fact, different isotopes produce somewhat different energies, but the value used here is a good-enough approximation for the present purpose.
[19] The International Nuclear Safety Center, operated by the Argonne National Laboratory, maintains a list of registered nuclear reactors worldwide. Prof. John Learned of the University of Hawaii, Manoa obtained a text version of the list through private channels.